

Numerical Simulation of an Electrostatic Precipitator

Anandkumar S Malipatil
Department of Thermal Power engg.
Visvesvaraya Technological University
Gulbarga, India

Vijaykumar V Nagathan
Department of Mechanical Engineering
BLDEA'S College of Engineering,
Bijapur ,India

ABSTRACT:- Optimization of the perforated plates of the electrostatic precipitator at the inlet section requires expensive testing with much iteration. A numerical analysis can be employed to reduce the number of design iterations. For power stations, the gas velocity is preferably between 1 m/s and 1.5 m/s in the treatment area, higher velocities tend to scour the collected dust (ash) off the plates. The required velocity is obtained by correcting the hole size of the perforated plates at the inlet section of the electrostatic precipitator. The present work describes the simulation of flue gas flow through an electrostatic precipitator and the optimization of the perforated plates of the electrostatic precipitator at the inlet section. A Finite volume approach has been used and the pressure-velocity coupling is resolved using the SIMPLE algorithm. In this numerical analysis perforated plates are considered as porous medium to simplify the solution. Comparisons are made between the available experimental results and the redesigned computational work. The experimental results show the velocity in the treatment area excess of 1.8 m/s, which is undesirable from efficiency point of electrostatic precipitator. Redesign of the perforated plates using computational work at the inlet part of the electrostatic precipitator, shows the velocity of flue gas in the treatment area of about 1.2m/s, which is more desirable.

NOMENCLATURE

U	Average velocity
ρ	Density of fluid
Re	Reynolds number
u	Absolute velocity
μ	Dynamic viscosity coefficient
ε	Turbulent energy dissipation
k	Turbulent kinetic energy
ϕ	Dissipation function
p	Pressure
C_2	Inertia Resistance coefficient
I	Turbulent intensity
D_h	Hydraulic Diameter
t	Thickness
A_p	Area of the plate (solid and holes)
A_f	Free area or total area of the holes

1. INTRODUCTION

There are various devices used for solid-gas separation in Power plants, such as

1. Gravitational Separators.
2. Bag house dust Collectors or Bag Filters.
3. Cyclone Separator.
4. Electrostatic Precipitator.

Of all the devices used for solid- gas separation, electrostatic precipitator finds wide application because of its inherent advantage over all other devices. Electrostatic precipitators can handle large volume of gases from which solid particulates are to be removed. Their technical superiority lies in low-pressure drop, high efficiency for small particles size, and relatively easy removal of the collected particulates [1].

Optimization of the Porous Plates of the electrostatic precipitator at the inlet and outlet section by experiment requires much time and it is expensive. A numerical analysis can be employ to reduce the number of design iterations. For electrostatic precipitator the flue gas velocity in the treatment area should be between 1 m/s and 1.5 m/s, higher velocities tend to scour the collected dust (ash) off the plates [2].

Computational fluid dynamics (CFD) is an attractive design tool to analyze the Fluid flow problems. Since it has the potential to explain the flow physics inside the electrostatic precipitator.

Presently the most widely used turbulence model in CFD codes is k- ε [3]. This model gives comprehensive results that are consistent with experimental data for most turbulent flows, and it is computationally less time and memory consuming than large eddy simulation (LES) and Detached eddy simulation (DES). The other approach is the Reynolds stress transport model RSTM that has a better accuracy than the k- ε model and requires less computational effort than LES and DNS.

2. COMPUTATIONAL MODEL

2.1. Governing Equations

Steady, incompressible, turbulent flows are governed by the Reynolds-averaged continuity and Navier-stokes

equations. The conservation forms of these equations in tensor notation can be written as follows:

Conservation of Mass:

$$\frac{\partial}{\partial x_j}(\rho U_j) = 0$$

Conservation of momentum:

$$\frac{\partial}{\partial x_j}(\rho U_i U_j) = \frac{\partial P}{\partial x_i} + \frac{\partial}{\partial x_j} \left[\mu \frac{\partial U_i}{\partial x_j} - \rho u_i u_j \right]$$

Where, U_i and u_i are the components of the mean and fluctuating velocities, P is the mean pressure, and ρ and μ are the fluid density and viscosity, respectively.

The numerical solution of the above set of mean equations is obtained by introducing additional transport equations for the Reynolds stresses represented by $\rho u'v'$. These equations introduce six variables and increase the difficulty of solving the system. Also, these equations contain higher order correlations which represent the processes of diffusion transport, viscous dissipation and fluctuating pressure-velocity interactions and have to be approximated by model assumptions in order to close the system of equations. The Reynolds stresses are calculated by using one of the following two turbulence models.

The standard k- ϵ model: The turbulent stresses are related to the mean velocity gradients via the turbulent viscosity, μ_t . This relationship is named as Boussinesq approximation [3].

The Reynolds Stress Transport Model: In the RSTM, the Reynolds stresses are calculated from their transport equations and the concept of an isotropic eddy viscosity is not required.

Table 1. Comparison of experimental and computational porosity values

Plates	Experimental Porosity values	Computational porosity values (Redesigned)
Inlet		
1	50%	40%
2	Upper 40%	Upper 40%
	Lower 40%	Lower 33%
3	Upper Left 23 %	Upper Left 23 %
	Upper Centre 33 %	Upper Centre 33 %
	Upper Right 23%	Upper Right 23%
Outlet		
4	Upper 40%	Upper 40%
	Central 23%	Central 23%
	Lower 40%	Lower 40%

The above table 1 shows the comparison of experimental and computational porosity values (redesigned porous plate).

2.2. Numerical Solution Procedure:

The mean flow, turbulence transport equations and porous media equations are solved numerically by using the FLUENT Code [5], which is a general-purpose solver for heat transfer and fluid flow in complex geometries and has been intensively validated against experimental data for many flow cases. The unstructured body fitted coordinates has been employed for meshing the complex geometry of a Electro static precipitator as in the present work. A finite-volume, non-staggered grid approach has been used and a second order upwind scheme is applied for the space derivatives of the advection terms in all transport equations. The pressure-velocity coupling is resolved by using the SIMPLE algorithm. Convergence of the solution is assumed when the sum of normalized residuals for each conservation equation is reduced to about 1×10^{-3} and the number of iterations is 997.

3. GEOMETRY AND BOUNDARY CONDITIONS

Fig 1 shows the electrostatic precipitator model employed in the present numerical work. The electrostatic precipitator model consists of inlet nozzle, treatment area, outlet nozzle and hopper. There are three perforated plates provided in the inlet nozzle, which are equally spaced. The entrance of the outlet nozzle is also provided with perforated plate.

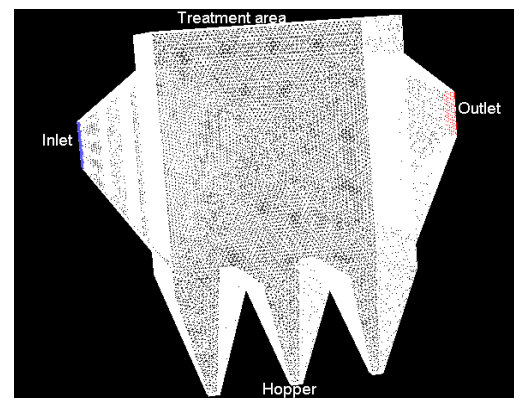


Fig.1. Mesh Model of an Electrostatic precipitator

Inlet velocity

$$\text{Designed gas volume m}^3/\text{hr} = 146124.$$

$$\text{Inlet area, m}^2 = 2.050 \times 1.320.$$

$$\text{Velocity} = \text{Volume} / \text{inlet area} = 146124 / (2.050 \times 1.320) \times 3600 = 15 \text{ m/s.}$$

$$\text{Inlet Temperature, } ^\circ\text{C} = 140.$$

Outlet Boundary conditions.

Pressure outlet

$$\text{Design pressure mmWc} = -300.$$

Table.2. Design parameter

DESIGN DATA		FUEL
SI #	Design parameter.	100% Indian coal.
1.	Design gas volume in m ³ /hr	146124
2.	Temperature °C	140
3.	Dust type	Boiler fly ash
4.	Maximum inlet dust loading gm/ Nm ³	10
5.	Outlet emission from ESP mg/ Nm ³	<=150
6.	Moisture in gas % V/V	9.19
7.	Unburnt carbon in flue gases, % W/W	10% assumed
8.	Collection area, m ²	1398.8
9.	Specific collection area m ² /m ³ / s	55.1
10.	Migration Velocity cm/s	7.62
11.	Design pressure mmWc	± 300
12.	Dust density for discharge Kg/ m ³	600

4. SOFTWARES USED

We used the Gambit as modeling software; it is flexible software for fluent solver. It has capability of producing fine surface. Fluent is used for the analysis of the model.

FLUENT provides complete mesh flexibility, including the ability to solve the flow problems using unstructured meshes that can be generated about complex geometries with relative ease. Supported mesh types include 2D triangular/ quadrilateral, 3Dtetrahedral/hexahedral/pyramid/wedge, and mixed (hybrid) meshes. FLUENT also allows refining or coarsening the grid based on the flow solution.

All functions required to compute a solution and display the results are accessible in fluent through an interactive, menu-driven interface[5].

5. RESULTS AND DISCUSSIONS

Introduction

This chapter represents the results of numerical simulation carried out to simulate the flow of flue gases passing through an electrostatic precipitator, in order to reduce the velocity of flue gases to prevent the scouring of the dust collected over the collector plates and to provide more retention time to absorb more dust.

The rectangular co-ordinate system was used for the presentation of the results

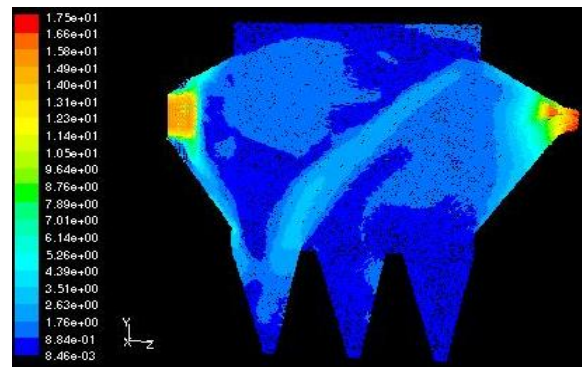


Fig.2. Velocity vector representing variation of flue gas velocity from Inlet to Outlet

Fig 2 shows the velocity variation of the flue gas passing through porous plate from the inlet of the electrostatic precipitator to the outlet in the longitudinal plane. At the inlet, the velocity of the flue gas was 15 m/s, from the above plot, the velocity at the treatment area varies from 0.8-1.76 m/s, and this is due to the screening of the gas flow by the porous plate. Some of the gas passes through the clearance provided at the bottom of the porous plate. The flow hits the first hopper and enters into the treatment area as shown in the fig. This flow will affect the uniform flow coming out from the porous plate.

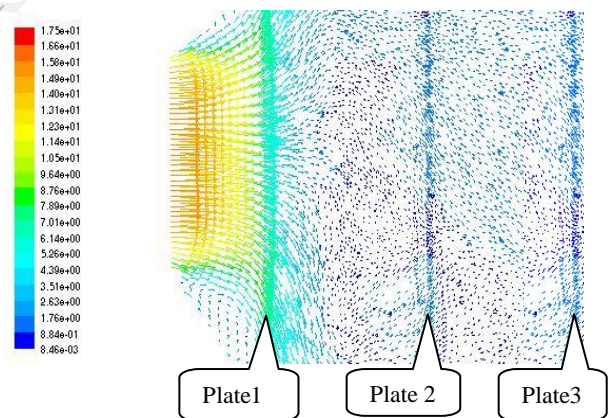


Fig.3. Velocity vector representing velocity at inlet to electrostatic precipitator

The velocity vector at the inlet section of the electrostatic precipitator shown in the fig 3. The inlet section contains three perforated plates at the equal intervals. The three porous plates, which are provided with different porosities. The first plate has the porosity value of 40 %. The second plate is split into two sections. The upper section has the porosity value of 40%, whereas the lower portion has 33% porosity value. The third plate is split into four sections; the upper left section has the porosity value of 23 %, the upper middle portion has the porosity value of 33 %, the upper right portion has the value of 23 %, the Bottom portion has the porosity value of 23 %. From the fig, the velocity at the end of the inlet section is 1.51 m/s.

Fig 4 shows the velocity vector at the treatment area including hoppers. The average velocity in the treatment area is 1.2 m/s, which is suitable for the efficient operation of the electrostatic precipitator.

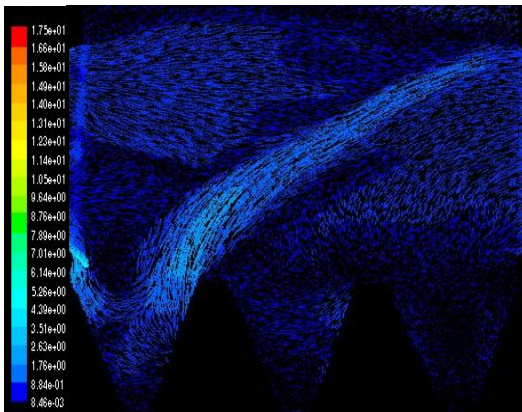


Fig.4. Velocity vector representing velocity at treatment Zone of electrostatic precipitator

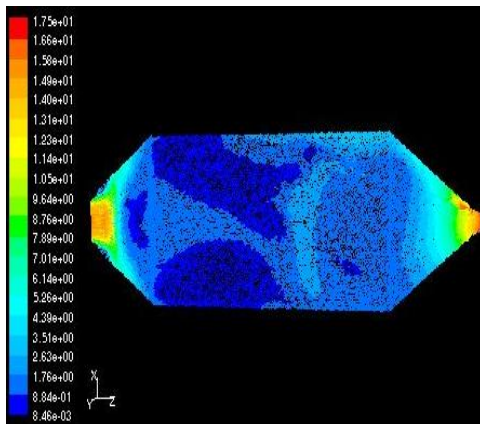


Fig.5. Velocity vector representing velocity at Inlet to outlet

Fig 5 shows the velocity vector at the sectional top view of the electrostatic precipitator, the flow hit the hopper and entering into the treatment area so that the velocity vector is not uniform.

The Velocity vector at the outlet portion is shown in the fig 6 the flow coming out the electrostatic precipitator without any recirculation with the velocity of 15 m/s.

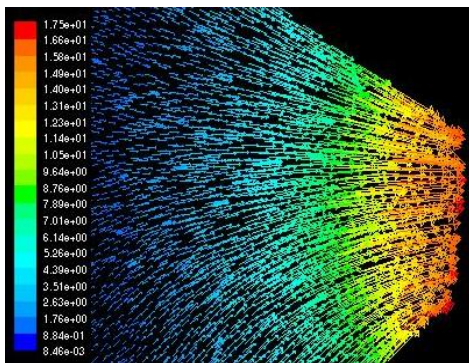


Fig.6. Velocity vector representing velocity at Outlet

Fig 7 shows the contour plot of velocity magnitude before and after plate one. The velocity before plate one was 8.125 m/s and after plate one, was 5.68 m/s. This is due to the screening of the flow.

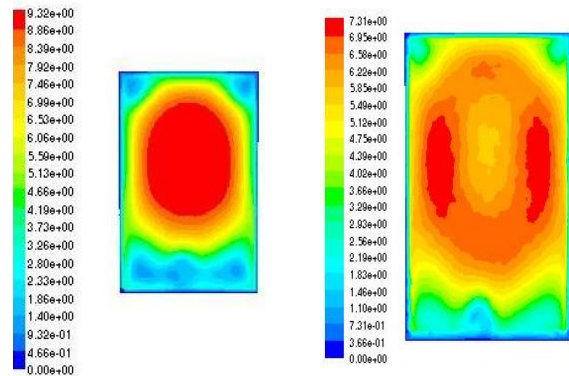


Fig.7. Contour plots of Velocity magnitude before and after plate 1

Fig 8 shows the contour plot of velocity magnitude before and after plate two, the velocity before plate two was 2.54 m/s and after plate two, was 2.15 m/s. This is due to the screening of the flow.

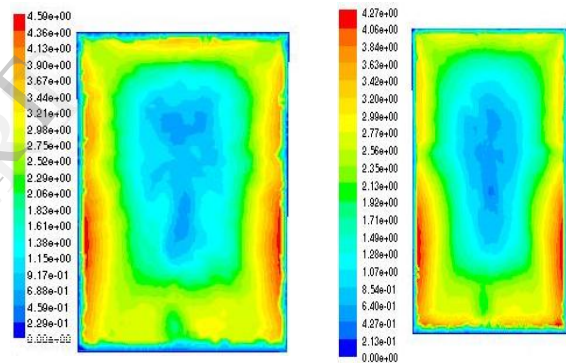


Fig.8. Contour plots of Velocity magnitude before and after plate

Fig 9 shows the contour plot of velocity magnitude before and after plate three, the velocity before plate three was 1.35 m/s and after plate, three was 1.32 m/s. This is due to the screening of the flow.

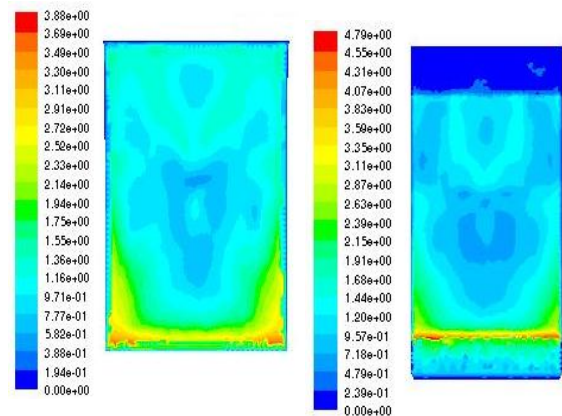


Fig.9. Contour plots of Velocity magnitude before and after plate 3

Fig 10 shows the contour plot of velocity magnitude in the treatment zones i.e. treatment zone one, two, three. From the contour plot of the treatment zone one, the velocity magnitude was found to be 0.79 m/s.

The velocity magnitude in the treatment zone two from the contour plots was found to be 0.95m/s.

Similarly, the velocity magnitude in the treatment zone three was found to be 0.88m/s.

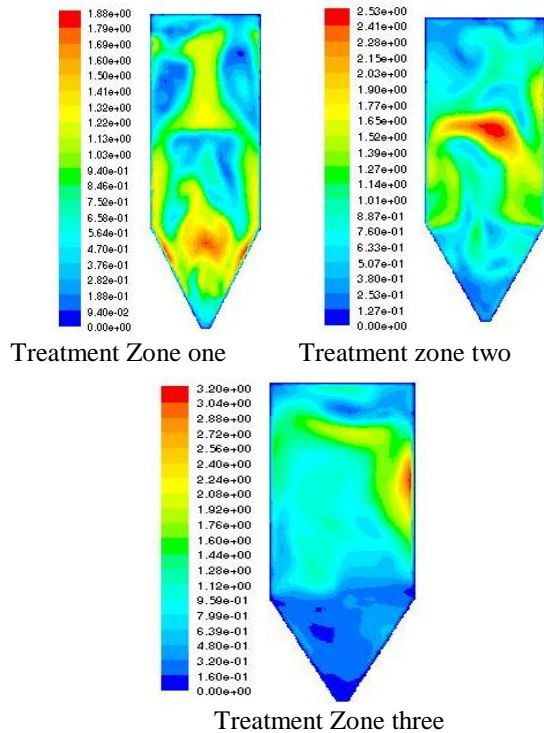


Fig.10. Contour plots of Velocity magnitude in treatment zone one, two and three

6. CONCLUSIONS

From this work the following conclusions are drawn

- A comprehensive literature survey has been carried out on the details of the electrostatic precipitator.
- Using the front-end commercial software Fluent, the finite volume model for the electrostatic precipitator was generated.
- Experimental results show the velocity in the treatment area of about 1.8–2.2 m/s. The numerical simulation result shows the velocity of 1.2m/s in the treatment area, which is more suitable for efficient operation of the electrostatic precipitator as shown in fig 5.3.
- From the results obtained the flow pattern were analyzed and important observations are mentioned. The flow hitting the first hopper as shown in fig 5.1 and enter into the treatment area which affect the uniform flow coming out from the perforated plates.

7. REFERENCES

- [1] Steam generator and auxiliaries -BHEL TRAINING MANUAL
- [2] GAN, G.H. and RIFFAT, S.B., (1997), "Pressure loss characteristics of orifice and perforated plates". *Exp. Therm. Fluid Sci.*, 14, 160-165..
- [3] H. K. Versteeg and W. Malalasekera "An introduction to computational fluid dynamics "The finite volume method, Longman Scientific & Technical Publication.
- [4] Fluent User Guide.
- [5] SKODRAS, G., KALDIS, S.P., SOFIALIDIS, D., FALTSI, O., GRAMMELIS, P. and SAKELLAROPOULOS, G.P., (2006), "Particulate removal via electrostatic precipitators - CFD simulation". *Fuel Process. Technol.*, 87, 623-631.

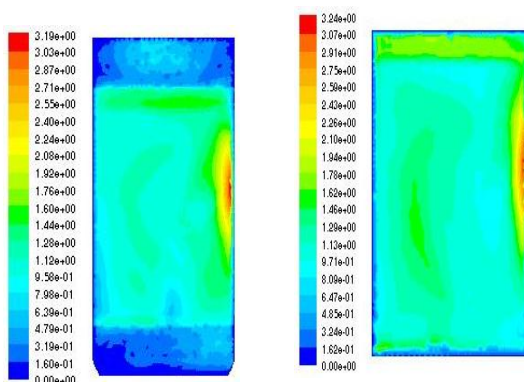


Fig.11. Contour plots of Velocity magnitude before and after plate four

Fig 11 shows the contour plot of velocity magnitude before and after plate, four. The velocity before plate four was 1.008 m/s and after plate, four was 1.25 m/s.